

Balancing pH and Yield: Exploring Itaconic Acid Production in *Ustilago cynodontis* from an Economic Perspective

Philipp Ernst

Forschungszentrum Jülich GmbH

Katharina Maria Saur

RWTH Aachen University

Robert Kiefel

RWTH Aachen University

Paul-Joachim Niehoff

RWTH Aachen University

Ronja Weskott

Forschungszentrum Jülich GmbH

Jochen Büchs

RWTH Aachen University

Andreas Jupke

RWTH Aachen University

Nick Wierckx (✉ n.wierckx@fz-juelich.de)

Forschungszentrum Jülich GmbH

Research Article

Keywords: *Ustilago cynodontis*, itaconic acid, low pH fermentations, downstream processing, techno-economic analysis

Posted Date: January 8th, 2024

DOI: <https://doi.org/10.21203/rs.3.rs-3830386/v1>

License: © ⓘ This work is licensed under a Creative Commons Attribution 4.0 International License.

[Read Full License](#)

Additional Declarations: No competing interests reported.

Abstract

Background: Itaconic acid is a promising bio-based building block for the synthesis of polymers, plastics, fibers and other materials. In recent years, *Ustilago cynodontis* has emerged as an additional itaconate producing non-conventional yeast, mainly due to its high acid tolerance, which significantly reduces saline waste coproduction during fermentation and downstream processing. As a result, this could likely improve the economic viability of the itaconic acid production process with Ustilaginaceae.

Results: In this study, we characterized a previously engineered itaconate hyper-producing *Ustilago cynodontis* strain in controlled fed-batch fermentations to determine the minimal and optimal pH for itaconate production. Under optimal fermentation conditions, the hyper-producing strain can achieve the theoretical maximal itaconate yield during the production phase in a low-density fermentation at pH 3.6, but at the expense of considerable base addition. Base consumption is strongly reduced at the pH of 2.8, but at cost of production yield, titer, and rate. A techno-economic analysis based on the entire process demonstrated that savings due to an additional decrease in pH control reagents and saline waste costs cannot compensate the yield loss observed at the highly acidic pH value 2.8.

Conclusions: Overall, this work provides novel data regarding the individual strain properties and production capabilities, contributing to a better understanding of the itaconic acid production process with *Ustilago cynodontis*, especially from an economic perspective.

Background

Itaconic acid (ITA) is considered as a promising renewable building block for the synthesis of plastics, synthetic resins, fibers and other materials (1–4). While itaconic acid and its derivatives also hold great potential in the medical and pharmaceutical sectors (5–7), a major opportunity exist in replacing acrylic acid and methacrylic acid in the polymer industry. However, this is only possible if the efficiency of the fermentation process can be increased to a point where it can compete with the petrochemical production (8, 9). In view of the already high yield, high titer, high productivity of the industrially well-established itaconic acid production process with the filamentous fungi *A. terreus* (10), the possibilities for further process improvements seem to be largely exhausted, requiring a qualitative breakthrough in other dimensions of the process window. Therefore, we focus on *Ustilago*, which with its stable yeast-like morphology, may enable such further efficiency gains in scaled up fermentation processes by providing greater degrees of freedom in handling of the fermentation broth (11, 12). These gains may be further boosted by utilizing untreated industrial feedstocks (13), as the substrate cost remains a critical factor in itaconic acid production (14). Moreover, the long history of safe use and lower biosafety level of *Ustilago* simplifies the itaconic acid production process in Europe compared to *A. terreus*.

In previous work, itaconate production with a deeply engineered *U. maydis* strain was optimized in terms of glucose feeding strategies (15). A continuous fed-batch fermentation with the reduced glucose baseline concentration enabled itaconate production at 100% of the theoretical maximal yield during the

production phase in a low-density fermentation. Since *U. maydis*'s pH sensitivity is largely uninvestigated, these fermentations were performed at a neutral pH. However, acidic pH values are beneficial for organic acid production (16, 17). Therefore, we investigated *U. cynodontis*, an additional natural itaconate producer that has recently been engineered to higher efficiencies (18, 19). The advantage of this strain lies in the amalgamation of yeast-like morphology with high acid tolerance, thus enabling both easier handling and the utilization of the benefits from lower process pH values. On the one hand, low pH values reduce bacterial growth, which generally reduces the risk of process contamination and may also allow to use a semi-sterile process, reducing costs. On the other hand, a low pH is crucial for downstream processing (DSP) efficiency (2, 20). Like other carboxylic acids, itaconic acid can be purified by various unit operations such as crystallization (2), extraction (21), adsorption, chromatography (22, 23), and membrane separation. Most of the itaconic acid purification techniques require the free acid. Therefore, the fully protonated state is required to obtain high yields during DSP (14, 21, 23–26). As a result, the pH needs to be lowered after fermentation by acid addition. In the industrially used crystallization, this leads to the formation of a co-salt with the base from the fermentation. While for *A. terreus*, this is not an issue due to its low fermentation pH, the concentration and composition of the co-salt limits the yield and increases the cost of waste disposal for *U. maydis* (14, 27). A techno-economic analysis already revealed that a slightly lower fermentation yield with *U. cynodontis* could be compensated by its low fermentation pH of 3.6 when compared to *U. maydis* (14). According to previous research, it is known that *U. cynodontis* is capable of producing itaconate even at pH values below 3.6 (19). Considering the pK_a values of itaconic acid (3.84 and 5.55), further reduction of the fermentation pH would shift itaconic acid dissociation towards the fully protonated species, significantly reducing the addition of pH control reagents and therefore costs. As a result, this could likely improve the economic viability of the itaconic acid production process with Ustilaginaceae.

A major factor in the establishment of *U. cynodontis* as a nonconventional itaconate producer was the deletion of *fuz7*, which arrested the cells in a yeast-like morphology thereby avoiding filamentous growth. Hosseinpour Tehrani, Saur et al. (19) determined the pH optimum for itaconate production at 3.6 with this morphology-engineered strain, but additional modifications were later performed to enhance itaconate production. These genetic modifications include the deletion of the P450 monooxygenase encoding *cyp3*, the overexpression of the transcription regulator *ria1*, and the heterologous overexpression of the mitochondrial tricarboxylate transporter *mttA* from *A. terreus*. Since this metabolic engineering altered the product spectrum and interfered with the regulation of the itaconate gene cluster, the pH optimum for itaconate production with this optimized strain may have shifted. In this study, we therefore investigated the itaconate production capabilities of the new itaconate hyper-producing *U. cynodontis* strain through controlled fed-batch fermentations. We identified the pH optimum of this strain and explored process window boundaries of key parameters such as the maximum itaconate titer and the lowest pH value possible. Additionally, the impact of pH on overall process economics was evaluated in a techno-economic analysis. Our findings revealed that additional cost savings could be achieved by minimizing pH control reagents and reducing saline waste. Although itaconate can be produced with the optimized *U. cynodontis* strain at pH values as low as 2.1, there is a clear optimum balance between key performance

indicators (KPI) that is not reached by simply maximizing individual parameters. In summary, this study provides insight into the specific characteristics and production capabilities of the new itaconate hyper-producing *U. cynodontis* strain, which improves our understanding of the itaconic acid production process with this microorganism, particularly from an economic standpoint.

Results and discussion

Comparison of *U. maydis* K14 and *U. cynodontis* ITA MAX pH for itaconate production at low pH values

Despite the advantage of acidic pH values for organic acid production, previous fermentations of *U. maydis* MB215 $\Delta cyp3 \Delta MEL \Delta UA \Delta dgat P_{ria1}::P_{etef} \Delta fuz7 P_{etef} mttA$ K14, henceforth named strain K14 for ease of reference, were performed at a neutral pH of 6.5 due to the largely uninvestigated growth- and production characteristics of this strain at lower pH values. In shake flask cultivations, engineered *U. maydis* hyper-producers do not grow at acidic pH conditions, but still produce significant amounts of itaconate at lower pH values (28, 29). Hence, itaconate production of *U. maydis* K14 was assessed in fermentations with different pH values for growth and itaconate production phase (Fig. 1A). To gain a comprehensive comparison, *U. cynodontis* NBRC9727 $\Delta fuz7 \Delta cyp3 P_{etef} mttA P_{ria1} ria1$, henceforth named strain ITA MAX pH for ease of reference, was cultured under similar conditions (Fig. 1B). To study the effect of reduced ammonium concentrations on the product to substrate yield in *U. cynodontis* ITA MAX pH, an additional low-density fed-batch fermentation was performed (Fig. 1C).

Until 72 h, both high-density fermentations behaved similarly (Fig. 1A, B). The depletion of nitrogen was achieved and itaconate accumulated to approximately 30 g L^{-1} . However, upon reaching lower pH levels, difference became apparent between the two species. In the case of you *U. maydis* K14, production almost completely stopped once the pH reached values below 4.0. On the contrary, *U. cynodontis* ITA MAX pH produced an additional 30 g L^{-1} itaconate after reaching acidic pH values. Remarkably, the *U. maydis* K14 culture did not even reach the final pH value 3.6, although the glucose concentration still declined until the end of the fermentation. This continued glucose uptake in the absence of further production indicates a very high metabolic energy demand for maintaining intracellular pH homeostasis. These results show that *U. maydis* K14 is not suitable to produce itaconate at lower pH values and is possibly more sensitive towards weak acid stress. Consequently, *U. cynodontis* ITA MAX pH was identified as a preferable candidate for subsequent characterization. If itaconic acid is to become a bulk chemical, yield is one of the most relevant production parameter because substrate cost is a decisive price-determining factor (14). The availability of nitrogen and the resulting C/N ratio offer a dimension to optimize the product to substrate yield by controlling the biomass density. Typically, lower nitrogen levels result in higher yields but also lower productivities (30). In previous fed-batch fermentations of *U. maydis* K14 with a reduced ammonium concentration, itaconate was produced at the maximal theoretical yield of $0.72 \pm 0.02 \text{ g}_{ITA} \text{ g}_{GLC}^{-1}$ during the production phase (15). A similar trend was observed for *U. cynodontis* ITA MAX pH during the low-density fermentation (Fig. 1C). This fermentation resulted in a similar itaconate titer of $67.8 \pm 0.7 \text{ g L}^{-1}$ compared to the high-density fermentation. Interestingly, the 5-fold

reduction in ammonium chloride as growth-limiting nutrient only resulted in an approximately 2-fold reduction of the maximum OD_{600} value as well as of the overall production rate ($0.22 \pm 0.01 \text{ g L}^{-1} \text{ h}^{-1}$). A similar phenomenon was observed for *U. maydis* (15). The lower substrate requirement for biomass production enabled a higher yield of $0.55 \pm 0.02 \text{ g}_{\text{ITA}} \text{ g}_{\text{GLC}}^{-1}$. When disregarding the glucose consumed during the first 24 hours in the growth phase, this fermentation achieved the theoretical maximal yield of $0.72 \pm 0.01 \text{ g}_{\text{ITA}} \text{ g}_{\text{GLC}}^{-1}$. This yield is the highest yield ever reported for *U. cynodontis*. Compared to previously published low-density pulsed fed-batch fermentation with a pH shift from 6.0 to 3.6, the fed-batch with continuous feed increased the titer by 62% and the yield by 41%, while the overall productivity remained nearly constant. These results clearly illustrate the benefit of a continuous glucose feed, preventing osmotic shocks caused by pulsed feeding. However, it is to note that the baseline glucose concentration during feeding was significantly higher than in the pulsed fed-batch fermentation. Although a higher osmotic stress due to elevated glucose concentration would be expected, it is also plausible that approximately 100 g L^{-1} glucose represents a threshold concentration for achieving more efficient itaconate production while maintaining relatively low osmotic stress. These findings are in line with those reported for itaconate production with *A. terreus*, where the highest yields were obtained at glucose concentration between 120 to 200 g L^{-1} (31). Almost the same is reported for citrate production in *A. niger* (32). This phenomenon should be further investigated for itaconate production with Ustilaginaceae.

Comparison of the itaconate production capabilities of *U. cynodontis* ITA MAX pH at neutral and acidic pH values

Previous research has demonstrated that *U. cynodontis* is also able to grow at the acidic pH value 3.6 (19). To investigate the impact of reduced pH values throughout the entire fermentation process, additional continuous fed-batch fermentations were conducted as described above. Growth and production capabilities achieved at pH 3.6 were compared to values obtained from fermentations at pH 6.5.

In the neutral pH fermentation, $64.7 \pm 10.5 \text{ g L}^{-1}$ itaconate was produced within approximately 160 h with an overall productivity of $0.40 \pm 0.06 \text{ g L}^{-1} \text{ h}^{-1}$ and the yield $0.42 \pm 0.02 \text{ g}_{\text{ITA}} \text{ g}_{\text{GLC}}^{-1}$ (Fig. 2B). Previous fed-batch fermentation with a pH-shift from 6.5 to 3.6 achieved similar KPIs (Fig. 1B). However, the low pH fermentation resulted in a higher itaconate yield of $0.49 \pm 0.01 \text{ g}_{\text{ITA}} \text{ g}_{\text{GLC}}^{-1}$ (Fig. 2A). In addition, the overall productivity was increased by 39% ($0.57 \pm 0.01 \text{ g L}^{-1} \text{ h}^{-1}$) and the titer by 22% ($79.2 \pm 1.3 \text{ g L}^{-1}$). These results show that *U. cynodontis* ITA MAX pH not only tolerates acidic conditions, it actually produces better at lower pH values. This result is promising, given that the acidic pH fermentation required approximately 3.5-fold less NOH compared to the neutral pH fermentation (112 mL and 398 mL 5 M NaOH solution). The KPIs are in good accordance with those previously achieved with this strain using a constant glucose feed controlled by an inline glucose sensor (78.6 g L^{-1} , $0.45 \text{ g}_{\text{ITA}} \text{ g}_{\text{GLC}}^{-1}$, $0.42 \text{ g L}^{-1} \text{ h}^{-1}$) (19). Less optimal progenitor strains of *U. cynodontis* ITA MAX pH are capable of producing itaconate even at pH levels below 3.6 (19). Given the pK_a values of itaconic acid of 3.84 and 5.55, further

reduction of the fermentation pH is expected to still significantly reduce base consumption (33). Thereby, costs associated with pH adjusting reagents can be further reduced. In addition, less hydrochloric acid (HCl) is necessary for DSP. This leads to a lower amount of co-salt in the fermentation broth, which can therefore be further concentrated which increases the crystallization yields. As shown by Saur et al. (14), this increased yield in DSP is able to compensate for partial yield loss in fermentation (cf. introduction). As a result, this capability holds the potential to improve the economic viability of the itaconic acid production process with *U. cynodontis*.

Identification of the pH optimum for itaconate production with *U. cynodontis* ITA MAX pH

The pH plays a crucial role as it determines the itaconic acid species distribution during the fermentation process. On the one hand, protonated itaconic acid negatively impacts the efficiency of the fermentation as it leads to weak acid uncoupling, which increases maintenance demand through energy-driven export of protons, and it possibly increases product inhibition by raising the intracellular itaconate concentration. On the other hand, the protonated acid greatly facilitates DSP as it avoids additional acid use and salt coproduction as described above. Therefore, it is crucial to carefully determine the optimum pH value in order to balance these effects and achieve the overall most efficient itaconate production. However, the pH optimum for itaconate production with *U. cynodontis* has so far only been determined with the sub-optimal production strain containing only the *fuz7* deletion. To examine the pH optimum of the new itaconate hyper-producing strain, a series of pH controlled fed-batch fermentations were conducted in standardized conditions. To avoid growth defects due to pH values below 3.6, the initial biomass production phase was performed at pH 3.6 for all fermentations. Following the depletion of the nitrogen source, the pH was allowed to drop to the corresponding lower pH value. To adjust the pH value above values of 3.6, NaOH was added.

During the initial biomass production phase, a similar growth was observed across all experiments. However, after the pH was adjusted to the corresponding value being tested, differences in the cell densities became apparent. pH values below 3.6 resulted in decreased optical densities (Fig. 3D), indicating acid stress of the cells. The stress is most likely caused by weak acid uncoupling, which is more prominent at low pH values due to higher fractions of the double-protonated species (Fig. 3A). The increased weak acid uncoupling at these lower pH values is also reflected in reduced yields (Fig. 3B). The lowest yield was observed at the minimal pH value of 2.1, which was identified in a batch fermentation without pH control during the itaconate production phase. However, the NaOH consumption during this fermentation was 36-fold reduced compared to the fermentation at pH 5.5 (Fig. 3C, Additional file 1). The highest yield with moderate base addition was achieved at pH 3.6, similar to what was previously determined for the morphology-engineered strain. The double-protonated form remained relatively constant within the pH range of 2.8 and 3.4, suggesting a potential inhibitory threshold for the cells (Fig. 3A). At pH 3.6, there is a significant reduction in H₂ITA. This reduction could explain the high KPIs observed at this pH value, indicating that H₂ITA concentrations are key to achieving maximum KPIs. Considering only the yield, the additional genetic modification did not change the pH optimum. The morphology-engineered strain also achieved the highest itaconate titer at 3.6, and showed afterwards

declining titer with increasing pH values. Regarding itaconate titers, it consequently appears that higher pH values negatively impact the regulation of the itaconate cluster genes of the *fuz7* variant. The new itaconate hyper-producing strain however, showed increasing titers with increasing pH values until a pH of 5.0 (Fig. 3A). This may be due to the interference in the regulatory mechanisms of the itaconate cluster genes by the *ria1* overexpression. The overexpression of *ria1* may have contributed to an increased tolerance of the strain towards higher product concentrations. It may also be possible that the overexpression of *ria1* reduced the pH dependency of the regulation of the itaconate cluster genes. One of the main potential benefits of production at more neutral pH values lies in the potentially higher titers (10, 33). In order to determine the maximum itaconate titer with this strain, an additional fed-batch fermentation was performed with a prolonged feeding phase.

In the fed-batch fermentation with a prolonged feeding phase, the itaconate titer kept linearly increasing up to 264 h up to approximately $92.3 \pm 10.7 \text{ g L}^{-1}$ at a rate of $0.34 \pm 0.01 \text{ g L}^{-1} \text{ h}^{-1}$ and a yield of $0.42 \pm 0.01 \text{ g}_{\text{ITA}} \text{ g}_{\text{GLC}}^{-1}$ (Fig. 4). During the remaining fermentation time, a linear increase of the itaconate titer could still be observed, however with a strongly reduced rate as the product inhibition became more and more prominent, taking another 434 h to produce only $32.9 \pm 4.0 \text{ g L}^{-1}$ additional itaconate. This fermentation reached a final itaconate titer of $125.2 \pm 14.6 \text{ g L}^{-1}$, one of the highest itaconate titers reported for Ustilaginaceae with NaOH titration. The itaconate concentration remained constant between 696 h and 720 h, indicating that the maximum titer was finally reached after approximately one month of fermentation time. In total, this fermentation resulted in an overall productivity of $0.17 \pm 0.02 \text{ g L}^{-1} \text{ h}^{-1}$ and a yield of $0.36 \pm 0.01 \text{ g}_{\text{ITA}} \text{ g}_{\text{GLC}}^{-1}$. Although a very high titer could be achieved through extended feeding, this came at the major expense of a lower yield end rate. Despite the reduced weak acid stress at the pH value of 5.0 and the higher itaconate production per cell, this fermentation highlighted the strong inhibitory effect of elevated product titers on the over KPIs, indicating a major efficiency loss at titers above $92.3 \pm 10.7 \text{ g L}^{-1}$ even at a higher pH value. This result highlights that not only elevated H_2ITA concentrations are inhibitory for the cells, but also higher overall product titers due to increased osmotic stress.

In summary, the engineered *U. cynodontis* ITA MAX pH strain shows an extended operational range for itaconate production compared to the previous morphology-engineered strain, particularly in terms of itaconate titers. The carbon balance of all fermentations is shown in Additional file 3. Analogous to the morphology-engineered strain, the achieved KPIs for the hyper-producing strain exhibited a moderate decrease at pH values below 3.6, which became more prominent at pH values below 3.0 (Fig. 3B). However, the volumes of NaOH added during these low-pH fermentations were also significantly reduced (Fig. 3C) and associated reductions in acid consumption and saline waste production during DSP can be expected. To assess whether these can economically compensate for the losses in fermentation yield at pH values lower than 3.6, an operational cost analysis was performed. We also added the economic results for fed-batch fermentations at higher pH values than 3.6 to provide a full picture of the cost structure changes.

Identification of the pH optimum by operative cost analysis

The process KPIs from the fed-batch fermentations served as an input parameter for the simulation. Those consist of product titer, fermentation yield, and pH during product formation phase (Fig. 3A, B). The results of the cost analysis are displayed in Fig. 5.

As expected, the simulated costs associated to acid and base use and saline waste disposal decrease with lower fermentation pH. Reduced amounts of HCl and saline waste could also be confirmed in crystallization experiments using real cultivation supernatants from batch fermentations (Additional file 4). However, those costs comprise only a small fraction of the total operational costs. Independent of the selected pH, the total operational costs are most strongly influenced by overall substrate yield. The outstanding fermentation yield at pH 3.6 cuts costs significantly while specific operational costs are visibly larger at high and low pH values due to the poor substrate to product conversion. This cannot be outweighed by higher DSP yields as at lower pH as discussed in Saur et al. (14). The specific operational costs of approximately 1.04 EUR kg⁻¹ at pH 3.6 achieved in this work are approximately 0.40 EUR kg⁻¹ lower than those previously obtained for this strain (14). Nevertheless, to successfully compete with the petrochemical production of the counterparts acrylic acid and methacrylic acid, it is necessary to further reduce the production costs (34).

Conclusion

From an economic perspective, the process pH should not be controlled below 3.6 as yield deficits cannot be counterbalanced by reduced amounts of salt waste production. However, lower pH values during the production phase may still offer advantages. Due to the further reduced risk of process contamination, semi-sterile industrial feedstocks might be fed during the production phase, reducing costs. The general feasibility to produce itaconate at the highly acidic pH value 2.8 using the side stream thick juice from the sugar industry could already be successfully demonstrated (Additional file 5). In addition *in situ* product removal is greatly facilitated by direct production of the protonated itaconic acid at these lower pH values (21, 35). Therefore, the low fermentation pH of 2.8 is expected to significantly enhance product removal efficiency, which may further reduce the DSP costs. These effects should be investigated in the future. Further studies could also comprise a techno-economic analysis excluding the initial biomass production phase since Hosseinpour Tehrani, Saur et al. (19) showed that *U. cynodontis* ITA MAX pH can be subjected to repeated batch fermentations. In this way, the same biomass could be used multiple times for itaconate production, potentially leading to a more improved cost analysis of the itaconate production process with Ustilaginaceae.

Overall, this study provides exquisite data regarding the production strain properties and production capabilities, potentially enabling the development and implementation of a more cost-effective itaconic acid production process with Ustilaginaceae in the future.

Materials and Methods

Chemicals and strains

All chemicals used in this study were obtained from Sigma-Aldrich (St. Louis, USA), Thermo Fisher Scientific (Waltham, USA), or VWR (Radnor, USA) and were of analytical grade. Thick juice was supplied by Pfeifer & Langen Industrie- und Handels-KG.

The strain *U. cynodontis* NBRC9727 $\Delta fuz7 \Delta cyp3 P_{etef}mttA P_{ria1}ria1$ (18) and the strain *U. maydis* MB215 $\Delta cyp3 \Delta MEL \Delta UA \Delta dgat P_{ria1}::P_{etef} \Delta fuz7 P_{etef}mttA_{K14}$ (15) were used in this study.

Bioreactor cultivations

Controlled fed-batch cultivations were performed in a DASGIP® Bioblock (Eppendorf, Germany). The process was controlled using the Eppendorf DASware® control software (Eppendorf, Germany). Vessels with a total volume of 2.3 L and a working volume of 1.0 L were used. All cultivations were performed in batch medium according to Geiser et al. (36) containing 0.2 g L⁻¹ MgSO₄·7H₂O, 0.01 g L⁻¹ FeSO₄·7H₂O, 0.5 g L⁻¹ KH₂PO₄, 1 g L⁻¹ yeast extract (Merck Millipore, Germany), 1 mL L⁻¹ vitamin solution, 1 mL L⁻¹ trace element solution and varying concentrations of glucose and NH₄Cl, as indicated. The vitamin solution contained (per liter) 0.05 g d-biotin, 1 g d-calcium pantothenate, 1 g nicotinic acid, 25 g myo-inositol, 1 g thiamine hydrochloride, 1 g pyridoxol hydrochloride, and 0.2 g para-aminobenzoic acid. The trace element solution contained (per liter) 1.5 g EDTA, 0.45 g of ZnSO₄·7H₂O, 0.10 g of MnCl₂·4H₂O, 0.03 g of CoCl₂·6H₂O, 0.03 g of CuSO₄·5H₂O, 0.04 g of Na₂MoO₄·2H₂O, 0.45 g of CaCl₂·2H₂O, 0.3 g of FeSO₄·7H₂O, 0.10 g of H₃BO₃ and 0.01 g of KI. During cultivation, the pH was kept constant at the corresponding value by automatic addition of 5 M NaOH or 1 M HCl. The DO was controlled at 30% by a cascade mode: first agitation 800–1200 rpm (0–40% DOT controller output); second air flow 1–2 vvm (40–80% DOT controller output); third oxygen 21–100% oxygen (80–100% DOT controller output). The cultivation was performed at 30°C. The bioreactor was inoculated to a final OD₆₀₀ of 0.75 from an overnight pre-culture grown in screening medium according to Geiser et al. (36) containing 50 g L⁻¹ glucose and 100 mM MES buffer. 0.5 mL Antifoam 204 (Sigma, A6426) was added in the beginning of the cultivation and afterwards every 24 h.

Analytical methods

Identification and quantification of products and substrates in the supernatants was performed using a High Performance Liquid Chromatography (HPLC) 1260 Infinity system (Agilent, Waldbronn, Germany) with an ISERA Metab AAC column 300 × 7.8 mm column (ISERA, Germany). Separation was achieved by using an isocratic elution program at a flow rate of 0.6 mL min⁻¹ and a temperature of 40°C with 5 mM sulfuric acid as a solvent. For detection, a diode array detector (DAD) at 210 nm and a refraction index (RI) detector was used. All samples were filtered with Rotilabo® syringe filters (CA, 0.20 µm, Ø 15 mm) and afterwards diluted with ddH₂O. Analytes were identified via retention time compared to corresponding standards. Data analysis was performed using the Agilent OpenLAB Data Analysis - Build 2.200.0.528 software (Agilent, Waldbronn, Germany). The ammonium concentration in culture samples was

determined using the colorimetric method after Willis et al. (37). 10 μL culture supernatant was combined with 200 μL reagent (8 g Na-Salicylate, 10 g Trisodiumphosphate, 0.125 g Na-Nitroprusside), followed by the quick addition of 50 μL hypochlorite solution. After color development occurred (at least 15 min at RT), absorbance at 685 nm was measured in a flat-bottomed MTP plate without lid using a spectrophotometer. Ammonium concentrations were calculated using a standard curve of ammonium. Cell densities were quantified by optical density measurement at 600 nm wavelength (OD_{600}) by use of cuvettes and a spectrophotometer. Samples were diluted appropriately with the respective medium to fall within the linear measuring range of the photometer between absolute values of 0.2 and 0.4. For CDW determination, 2 mL culture broth was centrifuged at maximum speed followed by drying the pellet for 48 h at 65°C and afterwards weighing it.

Process design and operative cost analysis

The presented cost analysis is performed based on the process design described by Saur et al. (14) for itaconic acid production with *Ustilago* species. The according flowsheet is illustrated by a block flow diagram in Additional file 6.

The fermenter is fed with a diluted glucose feed of 500 g L^{-1} . During itaconic acid formation, the pH is maintained by base addition. The broth is separated from the cells by sterile filtration. Afterward, the filtered broth is concentrated by evaporation up to an itaconic acid concentration of 350 g L^{-1} . The pH is then lowered by acid addition so that a pH of approximately 2.8 is attained after crystallization. In the cooling crystallizer, the temperature is decreased to 15°C at atmospheric pressure. To increase the itaconic acid yield in the DSP, the purification sequence is repeated. Water is further removed from the mother liquor by a second evaporator up to a concentration at which a co-crystallization of itaconic acid and inorganic salt in a second cooling crystallizer can just be avoided. The inorganic salt-containing liquid stream is subsequently disposed. However, the itaconic acid solid fractions are dissolved in water at 80°C to remove residual contaminants and increase the purity of the final itaconic acid crystals. The elevated temperature requires only moderate amounts of water for dilution and avoids large heat requirements for evaporation in succeeding process steps. To decolorize the dissolved itaconic acid stream, an activated carbon treatment is performed. Finally, the solution is fed to an evaporative crystallizer. The mother liquor is recycled and mixed with the filtered fermentation broth while the itaconic acid crystals are fed to a dryer.

The process design requires the use of $\text{Mg}(\text{OH})_2$ as base in the fermenter. The subsequent acidic pH shift in the DSP is performed with HCl to form the highly soluble co-salt MgCl_2 . To alleviate the experimental investigation, fed-batch fermentations conducted for this work are pH-controlled by 5 M NaOH solution instead of a $\text{Mg}(\text{OH})_2$ suspension, which easily causes blocking of small-diameter tubing.

The flowsheet is modeled using Aspen Plus (V11) (Aspen Technology, Inc., Bedford, MA, USA). Calculated material streams and energy demands are used for the cost analysis. The details of the modeling framework and pricing are outlined in Saur et al. (14).

Abbreviations

ITA

itaconic acid

MTM

modified Tabuchi medium

YEPS

yeast extract, peptone, sucrose medium

HPLC

high performance liquid chromatography

DSP

downstream processing

ISPR

in situ product removal

OD

optical density

CDW

cell dry weight

NaOH

sodium hydroxide

MES

2-(N-morpholino) ethane sulfonic acid

KPI

key performance indicators.

Declarations

Author contributions

PE and NW designed the study. PE and RW performed the fermentations on glucose. KMS performed the crystallization experiments. RK performed the operative cost analysis. PJN performed the batch fermentation on thick juice. NW supervised the study. PE and NW drafted the manuscript. PE, KMS, RK, PJN, RW, JB, AJ and NW revised and prepared the final version of the manuscript. All authors read and approved the final manuscript.

Funding

This project has received funding from the Bio-based Industries Joint Undertaking (JU) under the European Union's Horizon 2020 research and innovation program under grant agreement No 887711. The JU receives support from the European Union's Horizon 2020 research and innovation program and the Bio-based Industries Consortium.

Availability of data and material

All data generated or analysed during this study are included in this published article and its supplementary information files.

Acknowledgements

We thank Pfeifer & Langen Industrie- und Handels-KG for providing the thick juice. We thank all project partners for fruitful discussions.

Conflicts of interest

The authors declare that they have no competing interests.

References

1. Klement T, Milker S, Jäger G, Grande PM, Domínguez de María P, Büchs J. Biomass pretreatment affects *Ustilago maydis* in producing itaconic acid. *Microbial Cell Factories*. 2012;11(43).
2. Okabe M, Lies D, Kanamasa S, Park EY. Biotechnological production of itaconic acid and its biosynthesis in *Aspergillus terreus*. *Applied Microbiology and Biotechnology*. 2009;84(4):597-606.
3. Steiger MG, Wierckx N, Blank LM, Mattanovich D, Sauer M. Itaconic acid—an emerging building block. In: Wittmann C, Liao JC, editors. *Industrial Biotechnology: Products and Processes* 2017. p. 453-72.
4. Willke T, Vorlop KD. Biotechnological production of itaconic acid. *Appl Microbiol Biotechnol*. 2001;56(3-4):289-95.
5. Michelucci A, Cordes T, Ghelfi J, Pailot A, Reiling N, Goldmann O, et al. Immune-responsive gene 1 protein links metabolism to immunity by catalyzing itaconic acid production. *Proceedings of the National Academy of Sciences*. 2013;110(19):7820-5.
6. Mills EL, Ryan DG, Prag HA, Dikovskaya D, Menon D, Zaslona Z, et al. Itaconate is an anti-inflammatory metabolite that activates Nrf2 via alkylation of KEAP1. *Nature*. 2018;556(7699):113-7.
7. Olganier D, Farahani E, Thyrsted J, Blay-Cadanet J, Herengt A, Idorn M, et al. SARS-CoV2-mediated suppression of NRF2-signaling reveals potent antiviral and anti-inflammatory activity of 4-octyl-itaconate and dimethyl fumarate. *Nature Communications*. 2020;11(1):4938.
8. Klement T, Büchs J. Itaconic acid – A biotechnological process in change. *Bioresource Technology*. 2013;135:422-31.
9. Bafana R, Pandey RA. New approaches for itaconic acid production: bottlenecks and possible remedies. *Crit Rev Biotechnol*. 2018;38(1):68-82.
10. Hevekerl A, Kuenz A, Vorlop K-D. Influence of the pH on the itaconic acid production with *Aspergillus terreus*. *Applied microbiology and biotechnology*. 2014;98(24):10005-12.
11. Krull S, Lünsmann M, Prüße U, Kuenz A. *Ustilago Rabenhorstiana*—An Alternative Natural Itaconic Acid Producer. *Fermentation*. 2020;6(1):4.

12. Tabuchi T, Sugisawa T, Ishidori T, Nakahara T, Sugiyama J. Itaconic Acid Fermentation by a Yeast Belonging to the Genus *Candida*. *Agricultural and Biological Chemistry*. 1981;45(2):475-9.
13. Regestein L, Klement T, Grande P, Kreyenschulte D, Heyman B, Maßmann T, et al. From beech wood to itaconic acid: case study on biorefinery process integration. *Biotechnology for Biofuels*. 2018;11(1):279.
14. Saur KM, Kiefel R, Niehoff P-J, Hofstede J, Ernst P, Brockkötter J, et al. Holistic Approach to Process Design and Scale-Up for Itaconic Acid Production from Crude Substrates. *Bioengineering*. 2023;10(6):723.
15. Becker J, Tehrani HH, Ernst P, Blank LM, Wierckx N. An Optimized *Ustilago maydis* for Itaconic Acid Production at Maximal Theoretical Yield. *J Fungi (Basel)*. 2021;7(1).
16. van Maris AJA, Konings WN, van Dijken JP, Pronk JT. Microbial export of lactic and 3-hydroxypropanoic acid: implications for industrial fermentation processes. *Metabolic Engineering*. 2004;6(4):245-55.
17. Roa Engel CA, van Gulik WM, Marang L, van der Wielen LAM, Straathof AJJ. Development of a low pH fermentation strategy for fumaric acid production by *Rhizopus oryzae*. *Enzyme and Microbial Technology*. 2011;48(1):39-47.
18. Hosseinpour Tehrani H, Tharmasothirajan A, Track E, Blank LM, Wierckx N. Engineering the morphology and metabolism of pH tolerant *Ustilago cynodontis* for efficient itaconic acid production. *Metabolic Engineering*. 2019;54:293-300.
19. Hosseinpour Tehrani H, Saur K, Tharmasothirajan A, Blank LM, Wierckx N. Process engineering of pH tolerant *Ustilago cynodontis* for efficient itaconic acid production. *Microbial Cell Factories*. 2019;18(1):213.
20. Magalhães AI, de Carvalho JC, Thoms JF, Medina JDC, Soccol CR. Techno-economic analysis of downstream processes in itaconic acid production from fermentation broth. *Journal of Cleaner Production*. 2019;206:336-48.
21. Eggert A, Maßmann T, Kreyenschulte D, Becker M, Heyman B, Büchs J, Jupke A. Integrated in-situ product removal process concept for itaconic acid by reactive extraction, pH-shift back extraction and purification by pH-shift crystallization. *Separation and Purification Technology*. 2019;215:463-72.
22. González MI, Álvarez S, Riera FA, Álvarez R. Purification of Lactic Acid from Fermentation Broths by Ion-Exchange Resins. *Industrial & Engineering Chemistry Research*. 2006;45(9):3243-7.
23. Ortíz-de-Lira A, Reynel-Ávila HE, Díaz-Muñoz LL, Mendoza-Castillo DI, Aminabhavi TM, Badawi M, Bonilla-Petriciolet A. Sustainable Downstream Separation of Itaconic Acid Using Carbon-Based Adsorbents. *Adsorption Science & Technology*. 2022;2022:7333005.
24. Holtz A, Görtz J, Kocks C, Junker M, Jupke A. Automated measurement of pH-dependent solid-liquid equilibria of itaconic acid and protocatechuic acid. *Fluid Phase Equilibria*. 2021;532:112893.
25. Biselli A, Echtermeyer A, Reifsteck R, Materla P, Mitsos A, Viell J, Jupke A. Investigation of the elution behavior of dissociating itaconic acid on a hydrophobic polymeric adsorbent using in-line Raman

- spectroscopy. *Journal of Chromatography A*. 2022;1675:463140.
26. López-Garzón CS, Straathof AJJ. Recovery of carboxylic acids produced by fermentation. *Biotechnology Advances*. 2014;32(5):873-904.
 27. Gausmann M, Kocks C, Pastoors J, Büchs J, Wierckx N, Jupke A. Electrochemical pH-T-Swing Separation of Itaconic Acid for Zero Salt Waste Downstream Processing. *ACS Sustainable Chemistry & Engineering*. 2021;9(28):9336-47.
 28. Hosseinpour Tehrani H, Becker J, Bator I, Saur K, Meyer S, Rodrigues Lóia AC, et al. Integrated strain- and process design enable production of 220 g L⁻¹ itaconic acid with *Ustilago maydis*. *Biotechnology for Biofuels*. 2019;12(1):263.
 29. Becker J. Optimization of itaconic acid production by *U. maydis* through metabolic engineering & adaptive laboratory evolution: RWTH Aachen University, Doctoral Thesis; 2019.
 30. Zambanini T, Hartmann SK, Schmitz LM, Büttner L, Hosseinpour Tehrani H, Geiser E, et al. Promoters from the itaconate cluster of *Ustilago maydis* are induced by nitrogen depletion. *Fungal Biology and Biotechnology*. 2017;4(1):11.
 31. Karaffa L, Díaz R, Papp B, Fekete E, Sándor E, Kubicek CP. A deficiency of manganese ions in the presence of high sugar concentrations is the critical parameter for achieving high yields of itaconic acid by *Aspergillus terreus*. *Applied Microbiology and Biotechnology*. 2015;99(19):7937-44.
 32. Xu D-B, Madrid CP, Röhr M, Kubicek CP. The influence of type and concentration of the carbon source on production of citric acid by *Aspergillus niger*. *Applied Microbiology and Biotechnology*. 1989;30:553-8.
 33. Krull S, Hevekerl A, Kuenz A, Prüße U. Process development of itaconic acid production by a natural wild type strain of *Aspergillus terreus* to reach industrially relevant final titers. *Applied microbiology and biotechnology*. 2017;101(10):4063-72.
 34. Werpy T, Petersen G. Top Value Added Chemicals from Biomass: Volume I-Results of Screening for Potential Candidates from Sugars and Synthesis Gas. ; National Renewable Energy Lab., Golden, CO (US); 2004. Report No.: DOE/GO-102004-1992; TRN: US200427%%671 United States 10.2172/15008859 TRN: US200427%%671 NREL English.
 35. Pastoors J, Baltin C, Bettmer J, Deitert A, Götzen T, Michel C, et al. Respiration-based investigation of adsorbent-bioprocess compatibility. *Biotechnology for Biofuels and Bioproducts*. 2023;16(1):49.
 36. Geiser E, Wiebach V, Wierckx N, Blank LM. Prospecting the biodiversity of the fungal family Ustilaginaceae for the production of value-added chemicals. *Fungal Biology and Biotechnology*. 2014;1(1):2.
 37. Willis RB, Montgomery ME, Allen PR. Improved Method for Manual, Colorimetric Determination of Total Kjeldahl Nitrogen Using Salicylate. *Journal of Agricultural and Food Chemistry*. 1996;44(7):1804-7.

Figures

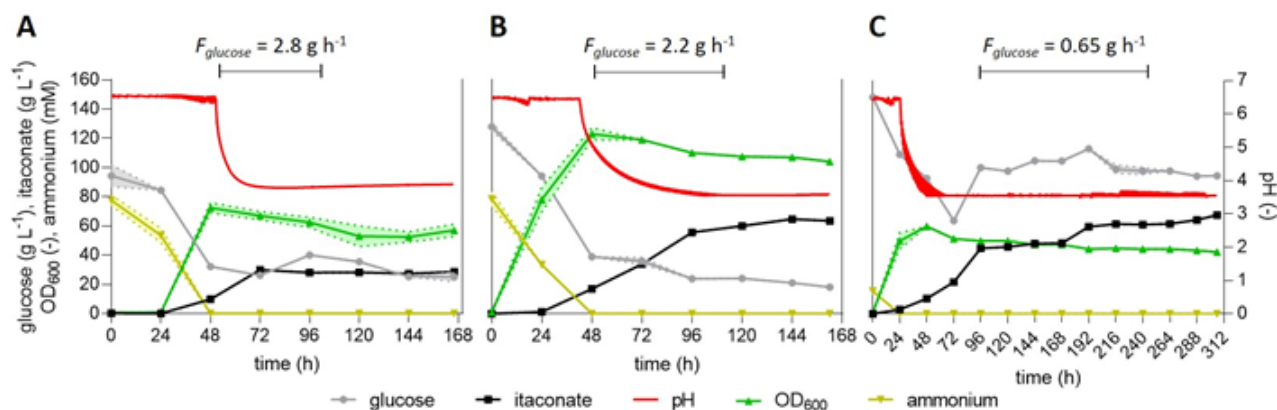


Figure 1: Fed-batch fermentations with continuous feed of *U. maydis* K14 with high ammonium concentration (A) and *U. cynodontis* ITA MAX pH with high (B) and low (C) ammonium concentration.

Concentration of glucose (●), itaconate (■), pH (red line), OD₆₀₀ (▲) and ammonium (▼) during fermentation in a bioreactor containing batch medium with approximately 120 g L⁻¹ glucose and 75 mM NH₄Cl. The pH was controlled by automatic titration with 5 M NaOH. After the depletion of nitrogen (24 h and 48 h), the pH was allowed to drop from pH 6.5 to pH 3.6 through the production of itaconate. Cultures were fed with an additional 130 g glucose (50 % w/v feeding solution) at a rate of 2.8 g h⁻¹ for *U. maydis* K14 and 2.2 g h⁻¹ or 0.65 g h⁻¹ for *U. cynodontis* ITA MAX pH during the indicated time interval. The feeding rates were estimated from glucose consumption rates of previous fermentations, aimed at keeping the glucose concentration at a relatively constant level of approximately 50 g L⁻¹. The low-density cultures were overfed between 72 h and 96 h. The mean values with standard deviation of two independent biological replicates are shown.

Figure 1

See image above for figure legend.

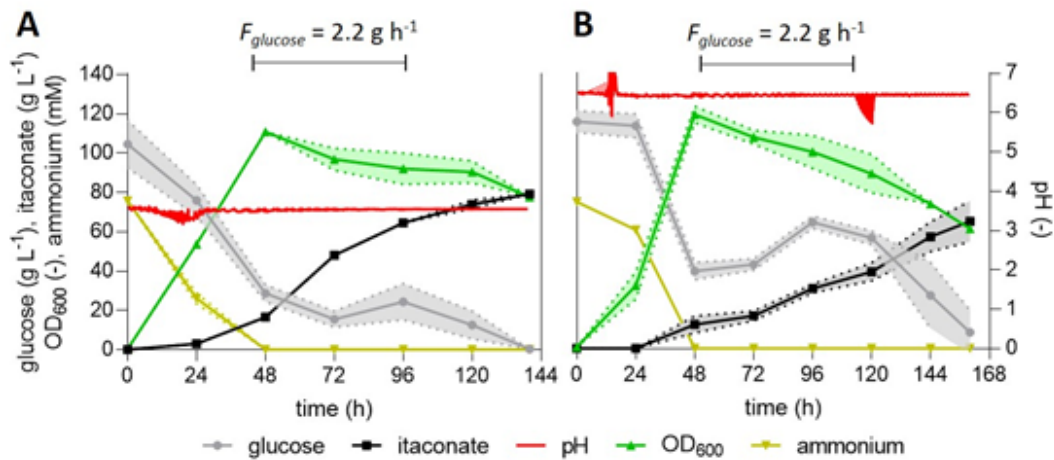


Figure 2: High-density fed-batch fermentations with continuous feed of *U. cynodontis* ITA MAX pH at pH 3.6 (A) and pH 6.5 (B).

(A, B) concentration of glucose (●), itaconate (■), pH (red line), OD_{600} (▲) and ammonium (▼) during fermentation in a bioreactor containing batch medium with approximately 110 g L^{-1} glucose and $75 \text{ mM NH}_4\text{Cl}$. The pH was controlled by automatic titration with 5 M NaOH . Cultures were fed with an additional 130 g glucose (50 \% w/v feeding solution) at a rate of 2.2 g h^{-1} during the indicated time interval. The feeding rates were estimated from glucose consumption rates of previous fermentations, aimed at keeping the glucose concentration at a constant level of approximately 50 g L^{-1} . The mean values with standard deviation of two independent biological replicates are shown.

Figure 2

See image above for figure legend.

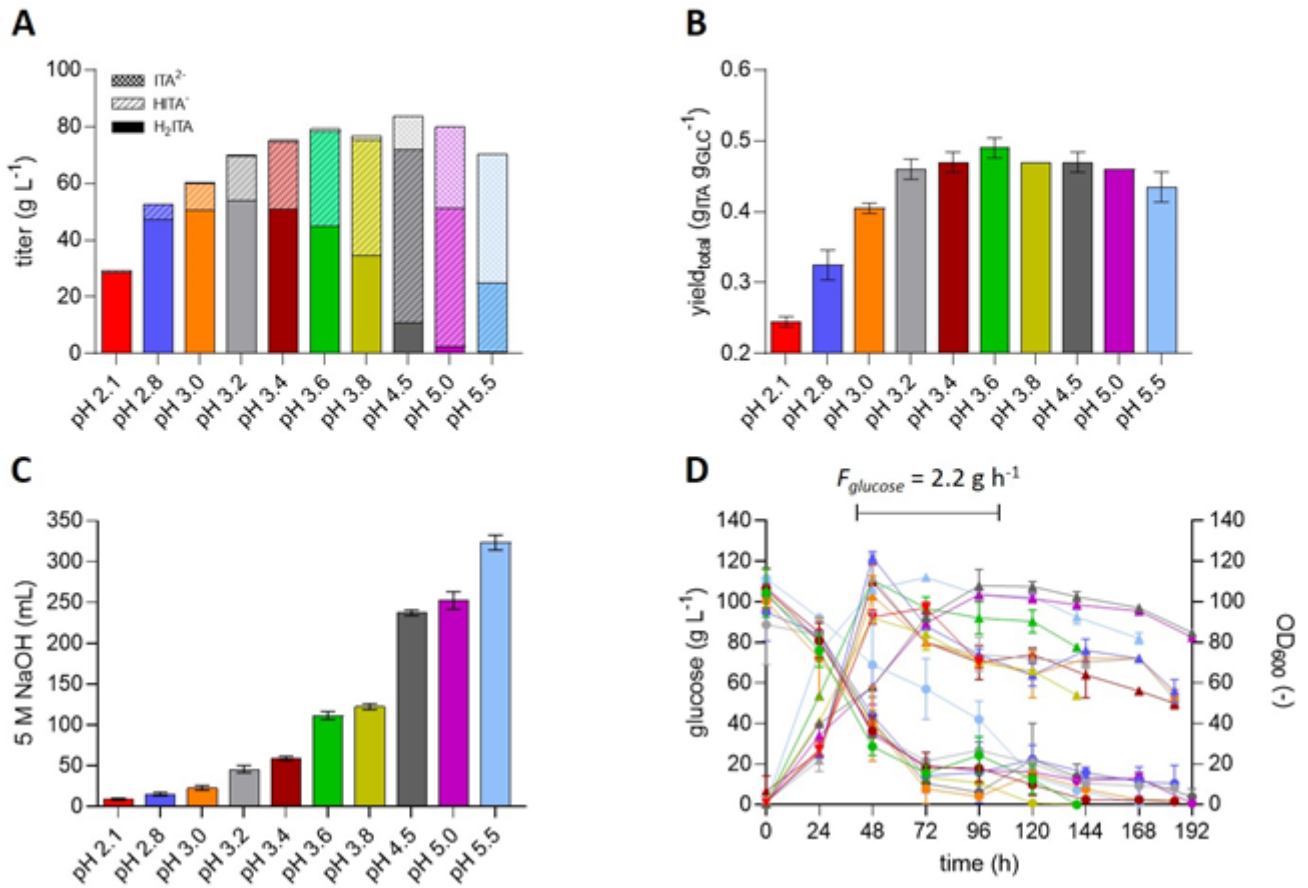


Figure 3

Fed-batch fermentations for the determination of the pH optimum for itaconate production with *U. cynodontis* ITA MAX pH.

(A) distribution of protonation states of itaconic acid, (B) yield_{total}, (C) added volumes of 5 M NaOH and (D) concentration of glucose (●) and OD₆₀₀ (▲) during fermentation at different pH values in bioreactors containing batch medium with approximately 110 g L⁻¹ glucose and 75 mM NH₄Cl. The colors in Figure D indicate fermentations at the pH values as shown in the panels A-C. The pH was controlled by automatic titration with 5 M NaOH. After the depletion of nitrogen (48 h), the pH was allowed to naturally drop to the corresponding lower pH value. pH values above 3.6 were manually adjusted with 5 M NaOH. pH 2.1 represents the lowest possible pH value that can be achieved with *U. cynodontis* ITA MAX pH. This pH value was determined in a high-density batch fermentation with approximately 200 g L⁻¹ glucose and an uncontrolled pH value during the production phase. All other cultures were fed with an additional 130 g glucose (50 % w/v feeding solution) at a rate of 2.2 g h⁻¹ during the indicated time interval in B. The mean values with standard deviation of two independent biological replicates are shown.

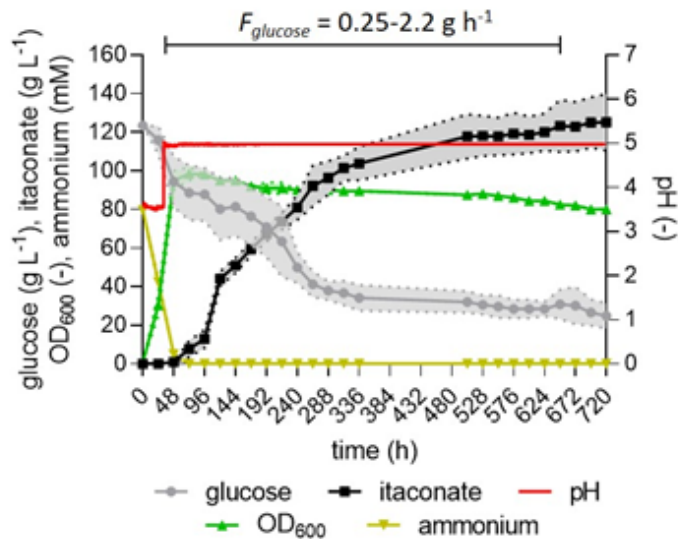


Figure 4: High-density fed-batch fermentation with a prolonged feeding phase of *U. cynodontis* ITA MAX pH. Concentration of glucose (●), itaconate (■), pH (red line), OD₆₀₀ (▲) and ammonium (▼) during fermentation in a bioreactor containing batch medium with approximately 120 g L⁻¹ glucose and 75 mM NH₄Cl. The pH was controlled by automatic titration with 5 M NaOH. After approximately 48 h, the pH was adjusted to pH 5 and afterwards maintained at this value until the end of the fermentation. Cultures were fed with an additional 540 g glucose (70 % w/v feeding solution) at rates between 0.25-2.2 g h⁻¹ during the indicated time interval. The feeding profile is shown in Additional file 2. The feeding rates were manually adjusted aimed at keeping the glucose concentration at a constant level of approximately 50 g L⁻¹. The mean values with standard deviation of two independent biological replicates are shown.

Figure 4

See image above for figure legend.

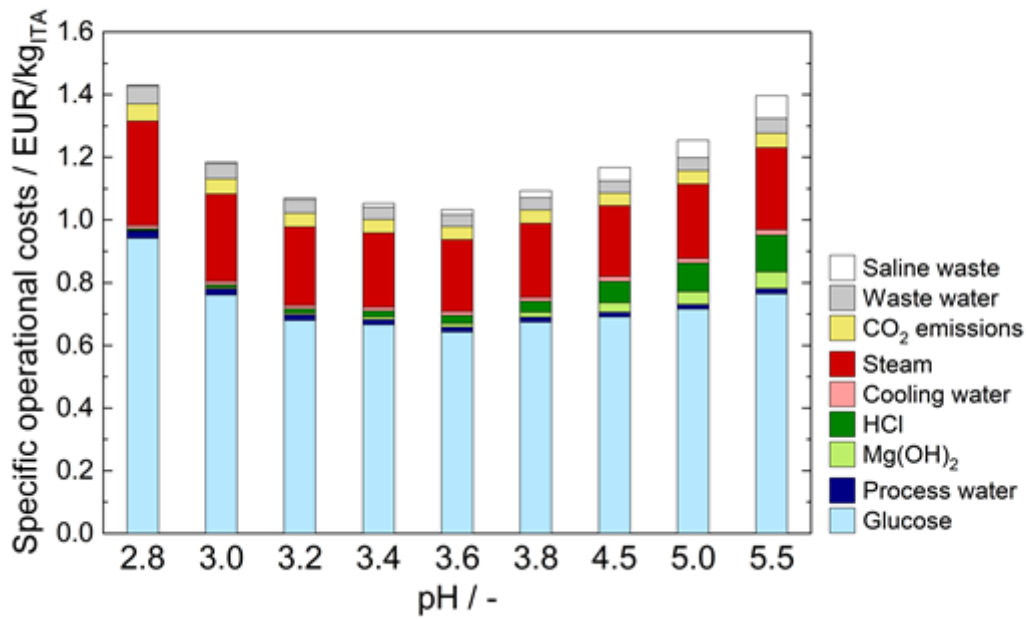


Figure 5

Specific operational costs for fed-batch fermentations at different pH values.

Supplementary Files

This is a list of supplementary files associated with this preprint. Click to download.

- [Additionalfilescombined.docx](#)